JTTEE5 6:109-115

Ti-6Al-4V/Hydroxyapatite Composite Coatings Prepared by Thermal Spray Techniques

K.A. Khor, C.S. Yip, and P. Cheang

The poor mechanical properties of hydroxyapatite (HA) can be enhanced by forming a composite with a bioinert and mechanically strong metal alloy such as Ti-6Al-4V. Biomedical composites composed of titanium alloys and HA can offer concomitant bioactive properties as well as good mechanical strength and toughness. This paper describes an attempt to improve coating mechanical properties by forming a composite composed of HA and Ti-6Al-4V. Several compositions (20, 33, and 80 wt% HA) were prepared. Subsequent examination of the plasma-sprayed coatings revealed alternating HA-rich and titanium-rich lamella microstructures. The HA-rich regions appeared porous as a result of poor interparticle adhesion, with the 80 wt% HA coatings having the highest porosity. Mechanical property analysis showed the 20 wt% HA coating to have the highest storage modulus (~60 GPa). This coating also had the highest bond strength (≥20 MPa max). The coatings tended to exhibit increased bond strength at thicknesses less than or equal to 60 μm. The excellent bond strength of the Ti-6Al-4V/HA composite is caused by the superior interfacial bond between the Ti-6Al-4V-rich splats and the substrate. The encouraging development of this composite raises the possibility of its use as a bond coat for plasma-sprayed HA on titanium-alloy implants.

Keywords bond strength, composite coating, hydroxyapatite, mechanical properties, microstructure, plasma spraying, Ti-6Al-4V

1. Introduction

BIOINERT metal alloys such as Cr-Co-Mo and Ti-6Al-4V have a long clinical history of implantation (Ref 1). The Ti-6Al-4V alloy in particular is popular for orthopedic application because of its high resistance to generalized and localized corrosion, good fatigue resistance, and biocompatibility. However, these materials lack the ability to bond chemically with bone, a property termed "bioactivity." In addition, the release of some metallic ions of aluminum and vanadium from the alloy may cause local irritation of the tissues surrounding the implant (Ref 2).

Recently, calcium phosphates such as hydroxyapatite (HA) have been deposited onto bioinert metallic implants to provide the necessary conditions for accelerated bonding with bony tissues and prevent the release of the metallic ions from Ti-6Al-4V (Ref 3-7). Hydroxyapatite is highly biocompatible and capable of direct chemical bonding with bone because of its chemical similarity to natural bone mineral. It has been applied as a coating on many types of implants, including hip and dental implants (Ref 8-11). Past studies have indicated that biological fixation of cementless hip prostheses achieves better bonding and negligible wear (Ref 12-14).

Hydroxyapatite also establishes strong interfacial bonds with titanium implants (Ref 15-17). However, HA can only be applied where the mechanical forces are low or only compressive (Ref 18). This property must be addressed for HA to reach its full potential as a biomaterial. One approach to overcome this problem is to form a composite between a mechanically strong bioinert, biocompatible metal alloy (Ti-6Al-4V) and the bioactive but mechanically fragile HA.

Ti-6Al-4V/HA composites can offer the bioactive property of HA combined with the excellent mechanical properties of titanium alloys for biomedical implants and prostheses. Several attempts have been made to fabricate Ti/HA composites in recent years. One approach is to produce a functionally graded material (FGM) that comprises titanium and HA combined by a powder metallurgical process (Ref 19). The different compositions are cold isostatically pressed before final consolidation by hot pressing. Another approach is to use hybridized pure Ti/HA powders as feedstock for plasma spraying in an argon atmosphere (Ref 20). Evaluation of the coating suggests that the HA dissociates from the feedstock mix during plasma spraying and coalesces to form individual lamellae. A FGM can also be formed using HA, a glass ceramic, and Ti-6Al-4V. Various compositions of the glass/HA layer are formed by slip coating. Encouraging osteointegration and osteoconduction characteristics have been reported (Ref 21).

This paper describes the preparation of Ti-6Al-4V/HA composite coatings by high-velocity oxyfuel (HVOF) and plasma spraying. The feedstock for the HVOF is prepared by mechanical alloying (MA), and the feedstock for the plasma spray process is prepared by mixing Ti-6Al-4V powders with a HA-based ceramic slurry. The process parameters involved are studied and the composites examined by scanning electron microscopy (SEM) and image analysis.

2. Experimental Materials and Methods

The HA powder was produced by reacting 0.5 *M* calcium hydroxide with 0.28 *M* orthophosphoric acid in a temperature-controlled bath (Ref 22). The resultant precipitate was dried at 180 °C, calcined at 800 °C for 4 h, and ground by using a mortar and pestle. Commercial Ti-6Al-4V powders, –100 mesh with a par-

K.A. Khor and **C.S. Yip,** School of Mechanical & Production Engineering, Nanyang Technological University, Singapore 63 9798, Singapore, mkakhor@ntuvax.ntu.ac.sig, FAX 65-791-1859; **P. Cheang,** School of Applied Science, Nanyang Technological University, Singapore 63 9798, Singapore.

ticle size range of 53 to 75 μm (Micron Co., Canada), were used in this study.

2.1 *Mechanical Alloying of Ti-6Al-4V/HA*

The Ti-6Al-4V and HA powders were milled in the Pulverisette 5 (Fritsch GmbH, Germany) planetary ball mill to form agglomerated clusters (Fig. 1) of 20 wt% HA. Milling of the Ti-6Al-4V/HA composite was carried out in an argon atmosphere to minimize oxidation of the titanium powders. Milling was performed over several durations and speeds, as shown in Table 1. These Ti-6Al-4V/HA aggregates were subsequently sprayed by a HVOF thermal spray system (HV 2000, Miller Thermal Inc., Appleton, WI, USA) onto roughened medium-carbon steel substrates. The HVOF spray parameters are listed in Table 2.

2.2 *Ceramic Slurry Mixing Method*

The second approach to preparing the Ti-6Al-4V/HA composite used a HA ceramic slurry to "coat" a layer of HA particles onto the Ti-6Al-4V powders. This approach has been employed successfully in the preparation of Al-Li-base metal-matrix composites with submicron SiC reinforcement (Ref 23). Figure 2 shows a schematic of the ceramic slurry mixing technique. The composite aggregates contain 20 wt% HA. Polyvinyl chloride (PVC) was added as binder (~1 wt%) for the ceramic powders. The composite powders were dried in vacuum (5.0×10^{-2} bar) at 120 °C and placed in a furnace to burn off (debind) the organic binder. After the composite powders were burned off at 550 to 600 °C, they were plasma sprayed (SG-100, Miller Thermal Inc., Appleton, WI, USA) onto Ti-6Al-4V substrates to form the composite coatings.

Table 3 lists the plasma spray parameters used in deposition of the Ti-6Al-4V/HA coatings. Some feedstocks were sprayed onto a prepared surface to specially produce peel-off coatings for porosity measurements by the mercury intrusion porosimetry (MIP) method.

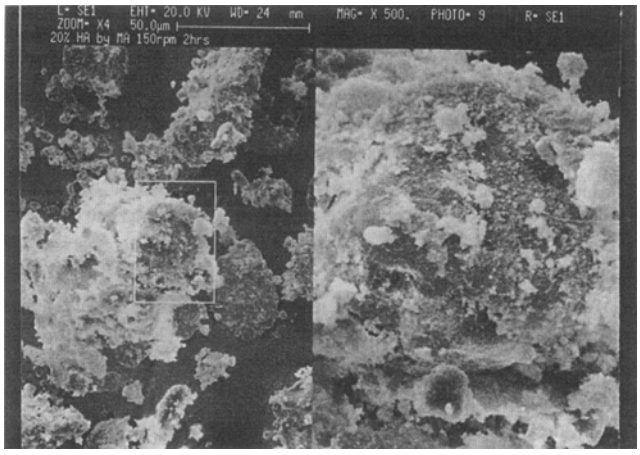

Fig. 1 Ti-6Al-4V/HA powder clusters formed after mechanical milling

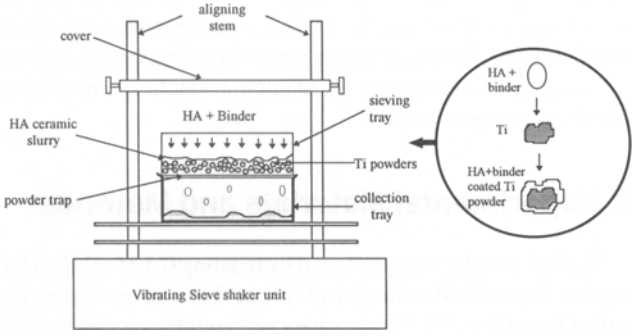

Fig. 2 Schematic of the ceramic slurry mixing technique for preparing Ti-6Al-4V/HA powder feedstock for plasma spraying

2.3 *Analytical Techniques*

Mechanical properties were measured using the Perkin Elmer 7-series dynamic mechanical analyzer (DMA). Each specimen was subjected to a static stress of 2.26 MPa, which was superimposed by a sinusoidal stress in the frequency range 0 to 20 Hz of magnitude 2.0 MPa. The Philips MHD 1880 analytical x-ray diffraction (XRD) system was used for phase characterization. The phase analysis was performed using nickel-filtered CuKα radiation at 45 kV and 30 mA. The 2θ range from 20° to 80° was covered at a continuous scan speed of 0.1°/min. Scanning electron microscopy was performed on the Cambridge Stereo scan S360 equipped with an energy-dispersive x-ray analyzer (Link AN 10/85S). Density measurements were performed with the Ultrapycnometer from Quantachrome.

3. Results

3.1 *HVOF Spraying of MA Powders*

The MA powder milled at 150 rev/min for 2 h was used for the HVOF spray as it has the least evidence of oxidation after the milling stage. The XRD pattern of the powders confirmed the presence of HA and Ti-6Al-4V and the absence of TiO_2 or any other form of oxides. The samples that were milled at high rates

Table 1 Operating parameters for mechanical milling of the Ti-6Al-4V/20 wt % HA composite powder

Sample	Time, h	Speed, rev/min
1	2	150
2	3	150
3	1	200
4	2	200
5	4	200
6	1	300

Table 2 HVOF spray parameters

Fuel gas, L/min	Hydrogen, 782
Primary gas, L/min	Oxygen, 272
Oxyfuel ratio	0.35
Total gas flow, L/min	1054
Powder wheel speed, rev/min	3.0
Standoff distance, μm	150-160
Coating thickness, μm	200

of revolution showed wide particle size distributions of approximately 1 to 90 μm. Samples 3 and 6 (milled for 1 h) showed evidence of nonuniform mixing of the HA and the Ti-6Al-4V.

Figure 3 shows the surface of the composite coatings prepared by HVOF using MA powders as the feedstock. The surface is characterized by fine, well-melted splats and small agglomerates composed of Ti-6Al-4V and HA particles. There is minimum spreading out of the feedstock upon impact on the substrate and no evidence of cracks. High-magnification observation of the as-sprayed surface showed surface pores in the size range of <1 to 2 μm. There was also evidence that the surface was composed of numerous pores and pore networks that arose from nonuniform melting of the feedstock. Moreover, some unmelted particles were likely the result of the lower flame temperature of the HVOF.

The polished cross section showed a predominantly dense structure. The coating obtained was thin (≤10 μm) as a result of the low deposition rate (~5 μm/min) and poor coating efficiency (<30% efficiency) of the HVOF when the MA powders were used as feedstock. Hence, additional passes were necessary, which greatly enhanced the oxidation of the Ti-6Al-4V. Difficulties were encountered in feeding the powder to the HVOF spray gun, likely due to the fineness of the MA powders. Laser diffraction particle size analysis revealed the size range to be predominantly in the <20 μm range.

3.2 *Microstructure of Plasma-Sprayed Ti-6Al-4V/HA Composite Coatings*

Figures 4 and 5 show the as-sprayed surfaces of plasma-sprayed Ti-6Al-4V/HA composite coatings with 20 and 80 wt% HA, respectively. The surface of the Ti-6Al-4V/20 wt% HA coating is characterized by undulated structures and smooth splats arising from a combination of partially melted and fully melted particles. Some cracking is visible on the splat surfaces, probably resulting from residual stresses upon rapid solidification. The Ti-6Al-4V/80 wt% HA coating surface in Fig. 5 contains granulated features and generally appears porous. The polished cross section shown in Fig. 6 reveals a typical lamellar structure consisting of alternating layers of Ti-6Al-4V and HA. Some unmelted particles are also visible. Observation at high magnification (3000×) revealed the HA-rich regions to be mechanically weak and also showed evidence of pullouts during polishing. In addition, some HA-rich lamellae had cracks, which must be "healed" for these composite coatings to exhibit enhanced mechanical strength.

The XRD patterns of the composite coatings are shown in Fig. 7. The 20 and 33 wt% HA coatings (Fig. 7a and b) contain predominantly titanium peaks and HA peaks. There is some evidence of amorphous HA after plasma spraying, as also confirmed by other investigators (Ref 24, 25), due to the loss of hydroxyl groups from the crystalline HA during plasma spraying. The 80 wt% HA coating (Fig. 7c) contains, in addition to crystalline HA and titanium peaks, α-TCP and CaO peaks resulting from the thermal decomposition of crystalline HA (Ref 26, 27).

Table 3 Plasma spray parameters for deposition of Ti-6Al-4V/HA coatings

Primary gas, psi	Argon, 50
Auxiliary gas, psi	Helium, 50
Anode	Forward feed
Cathode	Subsonic
Arc current, A	800
Arc voltage, V	30-32
Powder feed rate, rev/min	3.5 (~25 g/min)
Standoff distance, cm	12-14

Table 4 Average pore size and overall porosity of the Ti-6Al-4V/HA coatings

Coating	Average pore size, μm	Overall porosity, %
20 wt% HA	0.1676	19
33 wt% HA	0.4138	22.5
80 wt% HA	0.0542	24

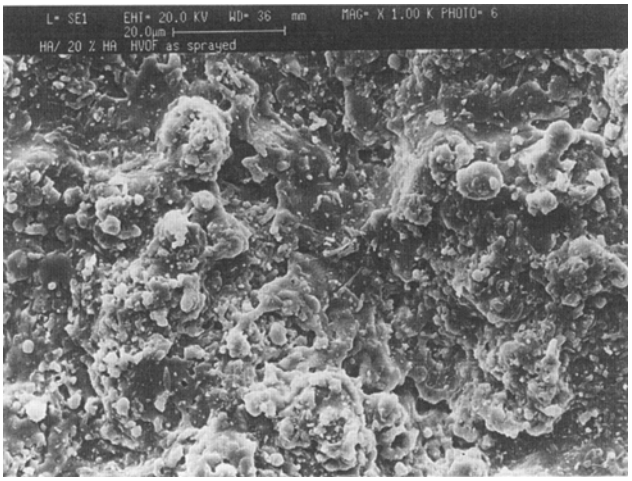

Fig. 3 As-sprayed surface of the Ti-6Al-4V/HA coatings deposited by HVOF

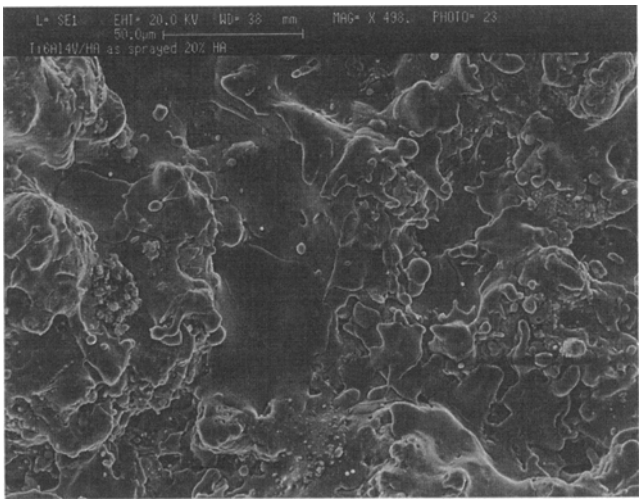

Fig. 4 As-sprayed surface of plasma-sprayed Ti-6Al-4V/20 wt% HA coating

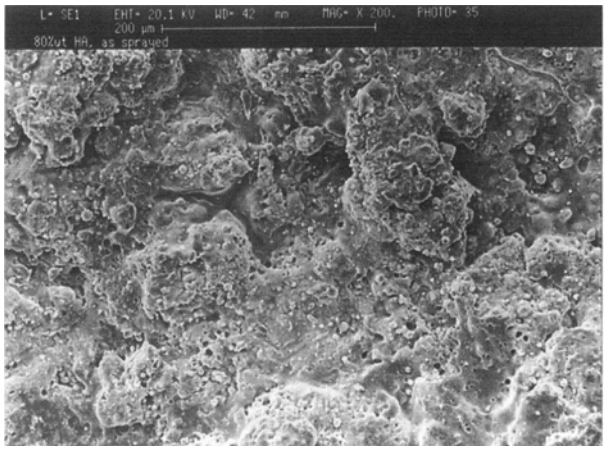

Fig. 5 As-sprayed surface of plasma-sprayed Ti-6Al-4V/80 wt% HA coating

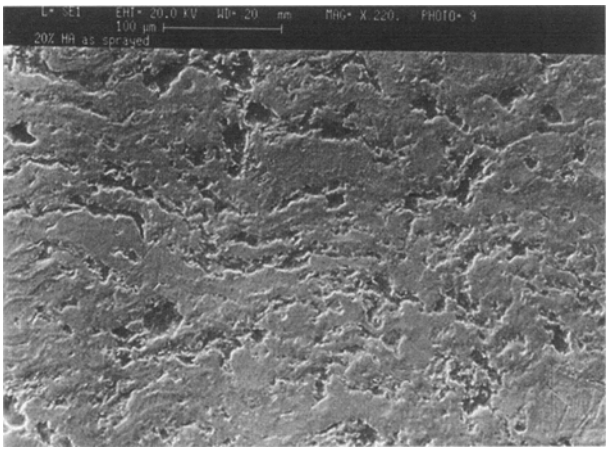

Fig. 6 Polished cross section of Ti-6Al-4V/HA coating

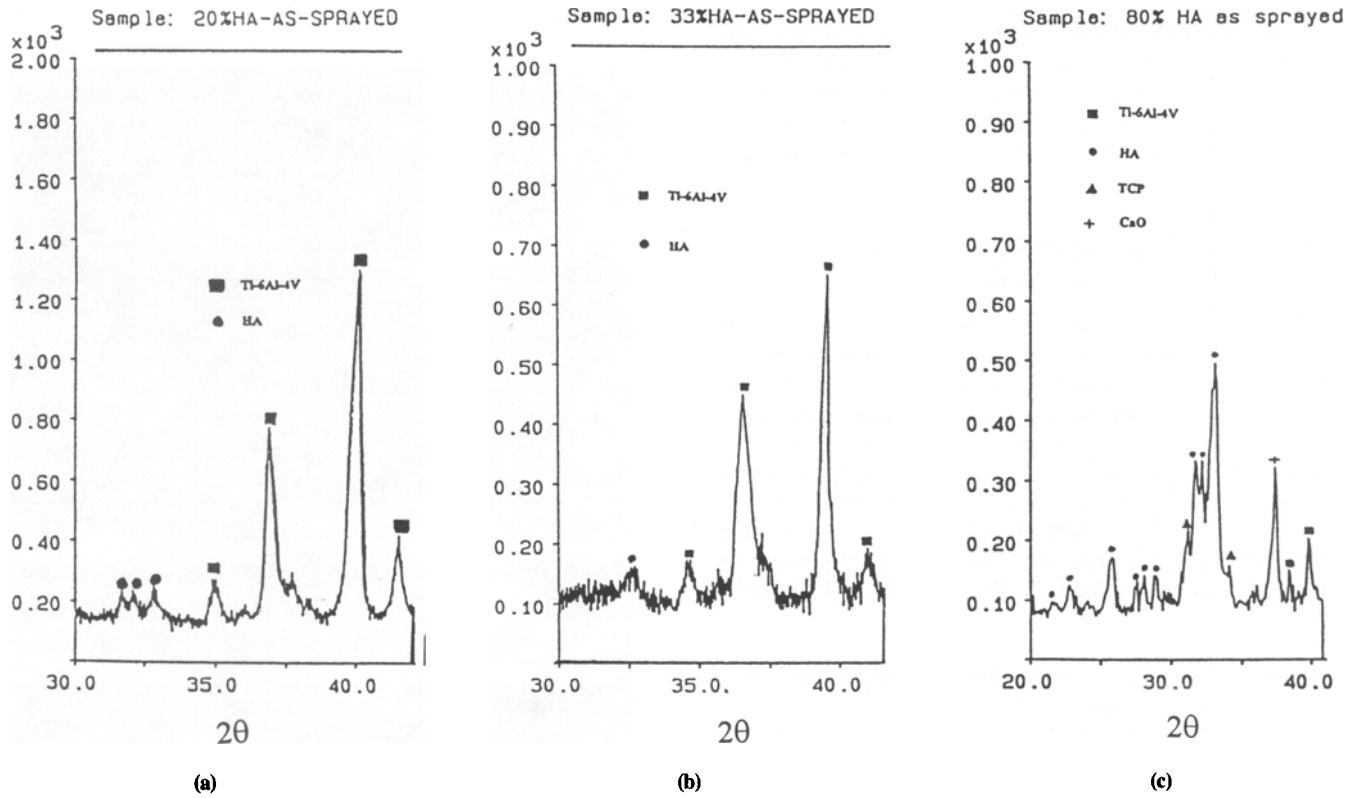

Fig. 7 XRD patterns of plasma-sprayed Ti-6Al-4V/HA coatings

3.3 *Tensile Bond Strength of Plasma-Sprayed Ti-6Al-4V/HA Composite Coatings*

Figure 8 shows the tensile bond strengths of plasma-sprayed Ti-6Al-4V/HA composite coatings (20 and 33 wt% HA), and Fig. 9 illustrates the tensile bond strength of Ti-6Al-4V/20 wt% HA in the as-sprayed state as a function of coating thickness. The samples were evaluated after heat treatment at 450 °C to relieve thermal residual stresses that accompanied the plasma spray process. The specific tensile bond strength of the coatings decreased progressively with coating thickness, with a dramatic drop observed in coatings thicker than 100 µm. Figure 8 shows that the 20 wt% HA composites possess better adhesion strength to the substrate than the 33 wt% HA composition.

Observation of the fractured surfaces by SEM showed evidence of brittle fracture and delamination of the coatings (Fig. 10). The higher specific bond strength of the 20 wt% HA composite coating is attributed to superior interfacial bonding with the substrate. There are, however, concerns that the high specific tensile bond strength readings for coatings with thicknesses of ≤60 µm could be attributed to epoxy glue penetrating through

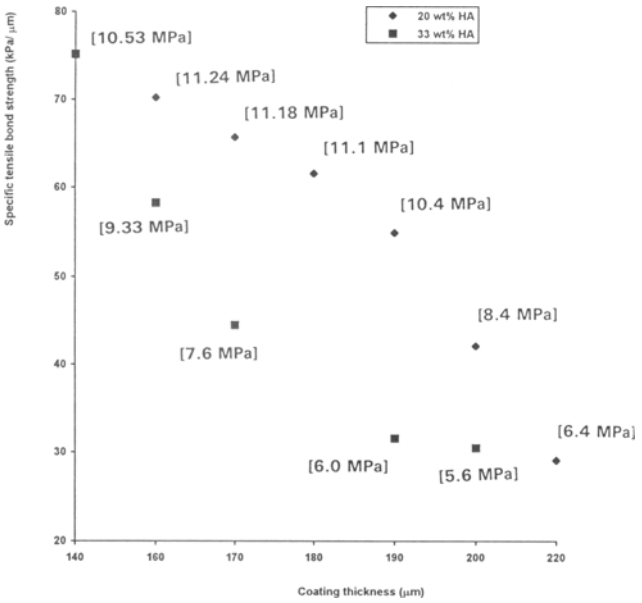

Fig. 8 Specific tensile bond strength of Ti-6Al-4V/HA (20 and 33 wt% HA) coatings. Note: Conventional bond strength values are bracketed.

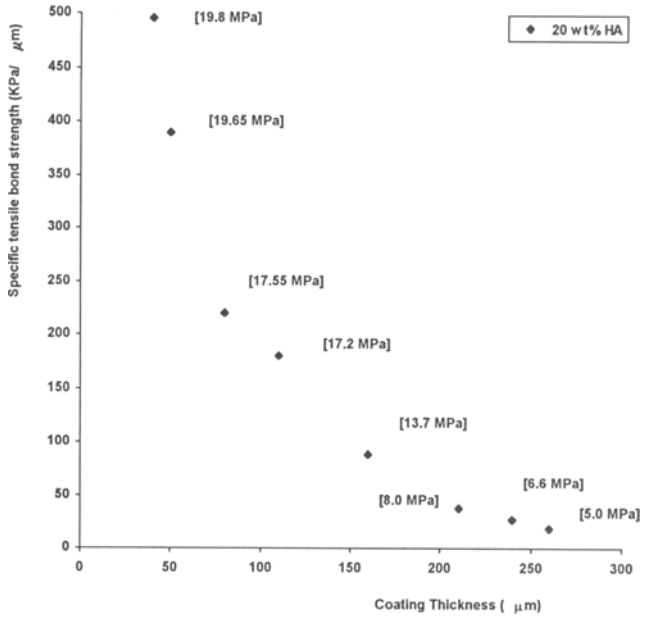

Fig. 9 Specific tensile bond strength of Ti-6Al-4V/20 wt% HA coatings as a function of coating thickness. Note: Conventional bond strength values are bracketed.

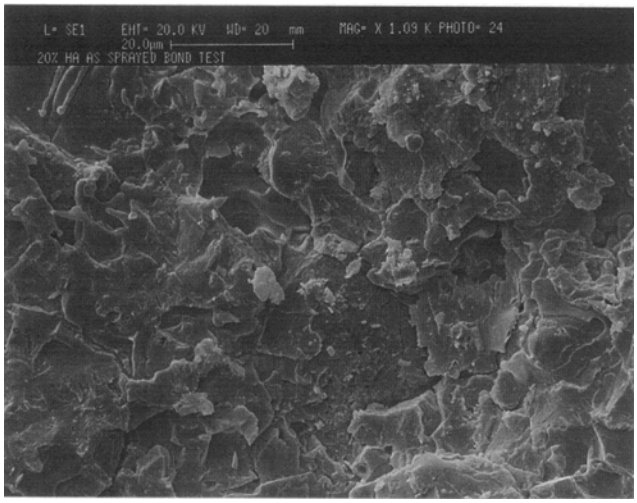

Fig. 10 Fractured surface of Ti-6Al-4V/HA coating after adhesive bond strength test

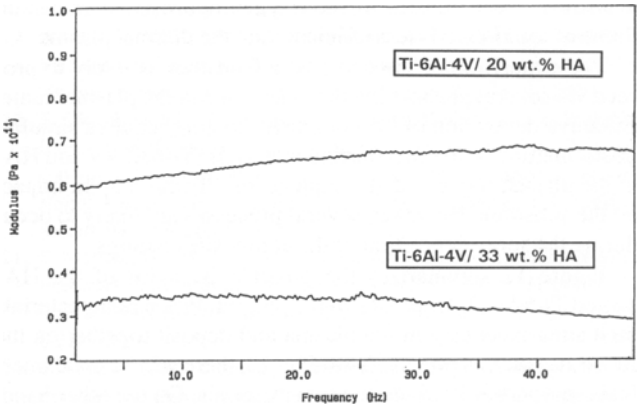

Fig. 11 Dynamic mechanical properties of Ti-6Al-4V/HA coatings

the porous coatings and hence artificially increasing the observed specific bond strength.

3.4 *Dynamic Mechanical Properties*

Figure 11 shows the DMA plots of the Ti-6Al-4V/HA composite coatings. The results indicate that the 20 wt% HA reinforced composite exhibits the highest modulus (~60 GPa), followed by the 33 wt% HA composite (~35 GPa). The modulus of Ti-6Al-4V is approximately 109 GPa, whereas sintered HA exhibit a modulus of approximately 90 to 120 GPa (Ref 28). It would therefore be expected that the sample with 33 wt% HA exhibit a lower modulus. The lower modulus (~35 GPa) of the composite with 33 wt% HA also indicates the poor interfacial and interlamellae properties of the coating.

3.5 *Porosity Measurement by Mercury Intrusion*

Table 4 lists the average pore diameter and overall porosity of the Ti-6Al-4V/HA coatings. The 33 and 80 wt% HA coatings exhibit the highest porosity (~22 to 24%). The average pore size of the 80 wt% HA coating is the lowest. This suggests that the pores that exist in the samples are among the partially melted HA particle "clusters." On the other hand, the pores in the 20 and 33 wt% HA samples are found at the ceramic/metal interface and around some partially melted Ti-6Al-4V particles. Subsequent processing by hot isostatic pressing (HIP) caused many of these interlamellae pores to close up, which would be expected to improve physical properties (Ref 29, 30).

4. Discussion

4.1 *Deposition of Ti-6Al-4V/HA Composite Coatings*

The deposition of the Ti-6Al-4V/HA composite coatings is influenced by the characteristics of the starting powders. The HVOF spraying of the composite coating is hampered by the fineness of the MA powders. Hence, it is difficult to deposit a coating that is reasonably thick (e.g., ~100 to 200 μm) for implant purposes. Such difficulties can be overcome by tailoring the MA process settings to produce larger composite feedstock for the thermal spray techniques in this study. The MA powders have also been fed to the plasma spray system, but the deposition is unsatisfactory due to choking of powder in the powder feed tube. Even when the powders do get sprayed in the plasma flame, the coating surface is not uniform and the overall coating thickness per torch pass is low.

The feedstock prepared by the ceramic slurry mixing technique is suitable for plasma spraying, at least from the powder flow point of view: Feed rate is uniform and choking of powders is minimal within the powder feed tube. Attempts have been made to use the ceramic slurry mixed feedstock for HVOF, but the particle sizes are too large for the powders to be effectively deposited. Heat transfer in the oxygen-hydrogen combustion flame of the HVOF is less efficient than the thermal plasma.

The deposition of the composite feedstock is likely to proceed via several phenomena that take place in the plasma flame. Effective deposition of the composite coating requires simultaneous melting of the two starting materials (Ti-6Al-4V and HA) in the plasma flame and subsequent solidification upon impact on the substrate. However, several processes are likely to occur during the spray deposition of the composite coatings.

Figure 12 summarizes the possible behavior of the HA-coated Ti-6Al-4V feedstock in the plasma. When both materials melt simultaneously in the plasma and deposit together on the substrate, such as process (a) in Fig. 12, there will be good interfacial properties between the two materials. On the other hand, if the Ti-6Al-4V/HA agglomerates melt partially, then the deposition will likely occur by process (b). However, it is also possible for the HA to detach from the Ti-6Al-4V surface and deposit independently, as shown in process (c). If the detached HA remains molten, then it will probably deposit on the coating as a lamella. Nevertheless, in such a case, there will be unsynchronized deposition of the metal and the ceramic, and the HA is likely to solidify ahead of Ti-6Al-4V.

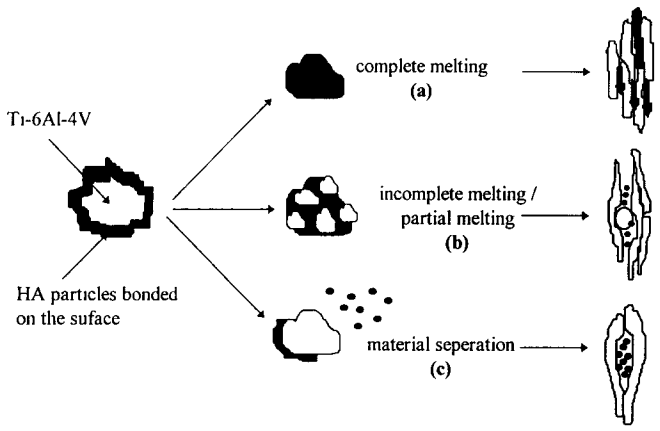

Fig. 12 Schematic of the deposition mechanisms involved in plasma spraying of Ti-6Al-4V/HA composite coatings

However, if the detached HA fragments in the plasma flame, which is very probable, then there will be pockets of HA clusters. This will result in poor interfacial properties between Ti-6Al-4V and HA. As a consequence, the HA-rich region will be characterized by loosely bonded particles, encased by Ti-6Al-4V splats. The Ti-6Al-4V-rich regions will contain a small amount of HA dispersed within the Ti-6Al-4V. The results will be poor interlamellae bonding, high porosity levels in the coatings, and a generally weak structure.

In view of the aforementioned phenomena involving separation of the HA from the Ti-6Al-4V particles in-flight during plasma spraying, future work will concentrate on mechanically "anchoring" the HA particles to the Ti-6Al-4V in the feedstock. The ceramic slurry mixing method does not bond HA strongly to the Ti-6Al-4V particles, because only the organic binder aids the adhesion of the two types of materials. The MA approach has the potential to solve this problem when the process parameters have been set to enable the HA particles to be embedded in the outer surface layer of the Ti-6Al-4V particles with no reduction in particle size. As found in this study, particle size reduction makes powder feeding difficult.

Subsequent treatment using HIP may be necessary to improve the mechanical properties of the coatings. The pores in the 20 and 33 wt% HA coatings probably are caused by the unmelted particles and poor interfacial adhesion of the Ti-6Al-4V phase and HA. In the 80 wt% HA coatings, however, the low average pore size value suggests that most of the pores are found in the HA "clusters." The considerable high porosity of the coatings contributes directly to their low mechanical strength. This is attributed to the poor interfacial relationship between HA and Ti-6Al-4V. Future work will concentrate on improving the powder preparation and thermal spraying parameters to enhance deposition of the two materials as a composite coating.

4.2 *Tensile Bond Strengths of the Ti-6Al-4V/HA Composite Coatings*

The tensile bond tests demonstrated that the 20 wt% HA coatings have higher adhesive strength than the 33 wt% HA coatings. This reflects the current processing difficulties in depositing the titanium alloy and HA uniformly. Microstructure observation in the SEM revealed pockets of HA-rich regions that are loosely bonded and wide gaps between the titanium alloy phase and the HA phase.

The bond tests also showed that the adhesive strength of the coatings is influenced by the overall coating thickness. High specific tensile bond strengths (~500 kPa/μm) have been recorded for coatings with thicknesses of ≤60 μm. There is a concern, however, that these high values result from epoxy penetration through the Ti-6Al-4V/HA coating. Nevertheless, the specific adhesive strength of the coatings in the range of 80 to 110 μm is higher than plasma-sprayed pure HA, and this composite can perhaps act as an effective bond coat for HA in Ti-6Al-4V implants. Current efforts focus on the adhesion of a plasma-sprayed HA layer on the Ti-6Al-4V/HA composites.

5. Conclusions

Ti-6Al-4V/HA composite coatings based on several compositions (20, 33, and 80 wt% HA) were prepared by thermal spray processes (plasma spray and HVOF). The coatings produced by the HVOF process used MA powders as feedstock. The coatings were thin (≤10 μm) and consistent feed of the fine powders through the rotor-wheel powder feeder was difficult.

The plasma-sprayed coatings were prepared with a different feedstock, a ceramic slurry mixing technique that coats the Ti-6Al-4V particles with HA. Subsequent examination of the plasma-sprayed coatings revealed alternating HA-rich and titanium-rich lamella microstructures, suggesting varying degrees of particle separation during the plasma spray process. Thus, the resultant microstructure was composed of HA-rich and Ti-6Al-4V-rich regions. The HA-rich regions appeared porous as a result of poor interparticle adhesion. The 20 wt% HA coating had the highest tensile adhesion bond strength (≥20 MPa for coatings ≤60 μm) and modulus (~60 GPa). The nature of the powder feedstock significantly influences the deposition process of the Ti-6Al-4V/HA coatings.

Acknowledgments

Financial assistance in the form of ARP 56/92 from Nanyang Technological University is gratefully acknowledged. The authors would like to thank Ms. Yong Mei Yoke, Mr. Alex Ng, and Mr. Sunny Lim for their technical assistance.

References

1. D.F. Williams, *Biocompatibility of Clinical Implant Materials*, CRC Press, 1981, chap. 2
2. H. Zitter and H. Plenk, Jr., The Electrochemical Behaviour of Metallic Implant Materials as an Indicator of Their Biocompatibility, *J. Biomed. Mater. Res.*, Vol 21, 1987, p 881
3. S.D. Cook, K.A. Thomas, J.E. Dalton, T.K. Volkman, T.S. Whitecloud, and J.F. Kay, Hydroxyapatite Coating of Porous Implants Improves Bone Ingrowth and Interface Attachment Strength, *J. Biomed. Mater. Res.*, Vol 26, 1992, p 989-1001
4. S.D. Cook, K. Thomas, J.F. Kay, and M. Jarcho, Hydroxyapatite Coated Titanium for Orthopaedic Implant Applications, *Clin. Orthop. Relat. Res.*, Vol 232, 1987, p 225-243
5. R.G.T. Geesink, K. de Groot, and C.P.A.T. Klein, Chemical Implant Fixation Using Hydroxyapatite Coatings, *Clin. Orthop. Relat. Res.*, Vol 225, 1987, p 147-170
6. J.A. Jansen, J.P.C.M. Van der Waerden, and J.G.C. Wolke, A Histological Evaluation of the Effect of Hydroxyapatite Coating on Interfacial Response, *J. Mater. Sci. Mater. Med.*, Vol 4, 1993, p 466-470
7. C.P.A.T. Klein, P. Patka, J.G.C. Wolke, J.M.A. de Blieck-Hogervorst, and K. de Groot, Long Term *In Vivo* Study of Plasma Sprayed Coatings on Titanium Alloys of Tetracalcium Phosphate, Hydroxyapatite and α-Tricalcium Phosphate, *Biomaterials*, Vol 15, 1994, p 146-150
8. R.G.T. Geesink, *Hydroxyapatite Coated Hip Implants: Experimental and Clinical Studies*, P. Ducheyne, T. Kokubo, and C.A. Van Blitterswik, Ed., Reed Healthcare Communications, Leidersdrop, 1992, p 121-138
9. P. Ducheyne and J.M. Cuckler, Bioactive Ceramic Prosthetic Coatings, *Clin. Orthop.*, Vol 276, 1992, p 102-114
10. R.G.T. Geesink, K. de Groot, and C.P.A.T. Klein, Bonding of Bone to Apatite-Coated Implants, *J. Bone Joint Surg.*, Vol 70-B, 1988, p 17-22
11. S.D. Cook, J. Enis, D. Armstrong, and E. Lisecki, Early Clinical Results with the Hydroxyapatite-Coated Porous Long-Term Stable Fixation Total Hip System, *Sem. Arthroplasty*, Vol 2, 1991, p 302-308
12. G.A. Lord, J.R. Hardy, and F.J. Kummer, An Uncemented Total Hip Replacement: Experimental Study and Review of 300 Madreporique Arthroplasties, *Clin. Orthop.*, Vol 141, 1979, p 2-16
13. M.B. Coventry, Historical Perspective of Hip Arthroplasty, *Joint Replacement Arthroplasty*, B.F. Morrey, Ed., Churchill Livingstone, 1991, p 491-499
14. T.W. Bauer, S.K. Taylor, M. Jiang, and S.V. Medendorp, An Indirect Comparison of Third-Body Wear in Retrieved Hydroxyapatite-Coated, Porous, and Cemented Components, *Clin. Orthop.*, Vol 298, 1994, p 11-18
15. R.G.T. Geesink, Hydroxyapatite-Coated Total Hip Prostheses: Two Year Clinical and Roentgenographic Results of 100 Cases, *Clin. Orthop.*, Vol 261, 1990, p 39-58
16. R.G.T. Geesink, K. de Groot, and C.P.A.T. Klein, Chemical Implant Fixation Using Hydroxyapatite Coatings: The Development of a Human Total Hip Prosthesis for Chemical Fixation to Bone Using Hydroxyapatite Coatings on Titanium Substrates, *Clin. Orthop.*, Vol 225, 1987, p 147-170
17. K. Søballe, E.S. Hansen, H.B. Rasmussen, P.H. Jorgenssen, and C. Bünger, Tissue Ingrowth into Titanium and Hydroxyapatite-Coated Implants during Stable and Unstable Mechanical Conditions, *J.Orthop. Res.*, Vol 10, 1992, p 285-299
18. J.F. Kay, Bioactive Surface Coatings for Hard Tissue Biomaterials, *CRC Handbook of Bioactive Ceramics, Vol II, Calcium Phosphate and Hydroxyapatite Ceramics*, T. Yamamuro, L.L. Hench, and J. Wilson, Ed., CRC Press, 1990, p 111-122
19. A. Bishop, C.Y. Lin, M. Navaratnam, R.D. Rawlings, and H.B. McShane, A Functional Gradient Material Produced by a Powder Metallurgy Process, *J. Mater. Sci. Lett.*, Vol 12, 1993, p 1516-1518
20. S. Oki, S. Gohda, T. Sohmura, T. Kimura, K. Ono, and T. Yoshioka, Preparation of Porous Spray Coating for Biomaterials with a Titanium-Calcium Phosphate Hybridized Powder, *Thermal Spray: International Advances in Coatings Technology*, C.C. Berndt, Ed., ASM International, 1992, p 447-451
21. S. Maruno, H. Itoh, S. Ban, H. Iwata, and T. Ishikawa, Micro-observation and Characterisation of Bonding between Bone and HA-Glass-Titanium Functionally Gradient Composite, *Biomaterials*, Vol 12, 1991, p 225-230
22. K.A. Khor and P. Cheang, Characterisation of Thermal Sprayed Hydroxyapatite Powders and Coatings, *J. Therm. Spray Technol.*, Vol 3 (No. 1), 1994, p 45-50
23. K.A. Khor, F.Y.C. Boey, Y. Murakoshi, and T. Sano, Granulation of Al Alloy Composite Aggregates for Cold Isostatic Pressing, *J. Mater. Process. Technol.*, Vol 37, 1993, p 431-439
24. Z. Zyman, J. Weng, X. Liu, X. Zhang, and Z. Ma, Amorphous Phase and Morphological Structure of Hydroxyapatite Plasma Coatings, *Biomaterials*, Vol 14 (No. 3), 1993, p 225-227
25. J. Weng, X. Liu, X. Li, and X. Zhang, Intrinsic Factors of Apatite Influencing Its Amorphization during Plasma Spray Coating, *Biomaterials*, Vol 16, 1995, p 39-44
26. S.R. Radin and P. Ducheyne, Plasma Spraying Induced Changes of Calcium Phosphate Ceramics Characteristics and Effects in In-Vitro Stability, *J. Mater. Sci. Mater. Med.*, Vol 3, 1992, p 33
27. D.P. Rivero, J. Fox, K. de Groot, and C.P.A.T. Klein, Calcium Phosphate-Coated Porous Titanium Implants for Enhanced Skeletal Fixation, *J. Biomed. Mater. Res.*, Vol 22, 1988, p 191-202
28. A. Ravaglioli and A. Kraejewski, *Bioceramics: Materials, Properties and Applications*, Chapman and Hall, London, 1992
29. K.A. Khor, Hot Isostatic Pressing Modification of Pore Size Distribution in Plasma Sprayed Coatings, *Mater. Manuf. Process., submitted for publication, 1996*
30. K.A. Khor and P. Cheang, unpublished results, 1996